Strains induced in carbon nanotubes due to the presence of ions: Ab initio restricted Hatree–Fock calculations

Shankar Ghosh, Vikram Gadagkar, A.K. Sood *

Department of Physics, Indian Institute of Science, Bangalore, Karnataka 560012, India

Abstract

Motivated by the experimental demonstration of the actuator action of single-walled carbon nanotubes and in situ resonance Raman experiments, we have performed ab initio restricted Hatree–Fock calculations of the electronic structure of a (5,5) single-walled nanotube in the presence of various ions. We show that the presence of ions near the nanotube causes combined axial and radial deformations of the nanotube. The presence of ions causes a small charge transfer from the ions to the nanotubes as well as changes the π–π overlap energy (γ). We find that the strains developed are primarily due to the electrostatic interactions with only a small contribution from the charge transfer.

1. Introduction

Single-walled carbon nanotubes (SWNT) have a large surface area [1–3] with all their π electrons in intimate contact with the environment. This makes both electronic and mechanical properties of nanotubes highly sensitive to the environment. It has been reported recently that the flow of various ionic and polar liquids generates voltage and current across SWNT samples [4]. It has been shown that small concentrations of gas molecules selectively change the conductivity of carbon nanotubes [5,6]. Nanotubes have also been reported to show actuator action [7], i.e., the variation of the nanotube length as a function of electrochemical bias. The nanotube actuator was found to respond to as high a frequency as 1 kHz. Raman spectroscopy [8–13] and optical electronic absorption [14] have both been used to probe the effect of various electrochemical environments on the electronic structure of nanotubes. It has been seen that the intensity of the radial Raman mode [8,13] changes non-monotonically as a function of applied bias.

There have been a number of theoretical attempts to explain the actuator action of nanotubes [15]. The key idea of these attempts is the proposal that the dimensional changes in the nanotubes are brought about by charge injection from the ions in the solution to the nanotubes. This effect is also used to explain the dimensional changes brought about in graphite intercalation compounds [16]. The main differences in these attempts is the way the additional charge interacts with the rest of the electronic system of the nanotubes [17,18]. However, in all these attempts the electrostatic interactions, over and above the doping effects, of the ions with the delocalized π electronic system of the nanotubes have not been taken into account. In the context of variation of the Raman intensity as a function of the electrochemical bias [8,12,13] two alternative proposals have been put forward. One explanation proposed by Ghosh et al. [8], invokes the tuning of the electronic band gap of the nanotubes by the changes in the π–π overlap energy (γ) due to the presence of ions near the nanotube surface. The other explanation proposes that the variation

* Corresponding author. Fax: +91 80 23602602.
E-mail address: asood@physics.iisc.ernet.in (A.K. Sood).

of the Raman intensity is due to the doping-induced change in the nanotube Fermi level and the related bleaching of the optical transitions [9–13].

It is the aim of this Letter to compare the relative importance of the two effects, i.e., (i) electrostatic interactions between the ions and the nanotube π electrons and (ii) the charge transfer from the ions to the nanotube, in developing strain in the nanotubes. To understand the variation of Raman intensity with electrochemical bias [8], we deduce the variation in the π–π overlap energy (γ) from the strains developed.

2. Calculation details

We have performed ab initio restricted Hatree–Fock (RHF) calculations using the GAMESS package [19]. Since, we are interested in the structural features of carbon nanotubes in the ground state, an atomic basis set of STO-3G orbitals for both the carbon atoms and the ions was chosen. The ions studied were Li^+, Na^+, K^+, Cl^-, Br^- and I^-. To allocate the distribution of the charge on the ions, the following algorithm was used. The nanotube-ions system, as shown in the inset of Fig. 1, was modelled by considering five unit cells of a (5,5) nanotube surrounded by two rings of ten ions each at a distance D from the nanotube surface. The total charge on the system was taken to be +20 for cations and −20 for anions. The length of the nanotube segment was about 11 Å and its diameter about 7 Å. The total number of atoms considered in the calculation was constrained by computational demands. The geometry of five unit cells of a (5,5) nanotube surrounded by two rings of ions is a simplified picture. In solution, the ions are hydrated [20]. However, the importance of the electrostatic interactions of the charged species with the delocalized π electrons of nanotubes in the development of strains would still be relevant in the modified hydrated ionic system. To start with, the ions were kept at D = 8 Å. At this distance there is a negligible overlap between the electronic wavefunction of the ions and the nanotube. Since the carbon atoms are more (less) electronegative than the cations (anions), the positive (negative) charge resides entirely on the cations (anions) at D = 8 Å. However, at lower D the electronic wave functions overlap resulting in a redistribution of the charge density. We analyze the partial atomic charges in terms of Mulliken charges. The self consistent field (SCF) convergence criterion was taken to be 10^{-8} for total energy changes and 10^{-5} for charge density changes between two consecutive cycles [21]. The optimization criteria for the convergence of a geometry search required the largest component of the gradient to be less than 0.008 nN, and the root mean square gradient to be less than 0.003 nN [19]. For all the calculations, the initial coordinates of the nanotube were those of a tube optimized in the absence of ions which is referred to as the pristine tube.

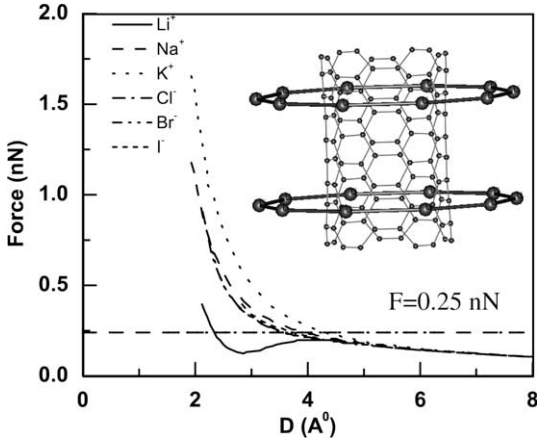

Fig. 1. Variation of the force acting on various ions (Li^+: solid line, Na^+: dashed line, K^+: dotted line, Cl^-: dashed-dotted, Br^-: dashed-dotted-dotted, I^-: short dash) as a function of D. The inset shows the geometry of the (5,5) nanotube and the ions used in the calculations.

3. Results

3.1. Distance of closest approach

To find the distance of closest approach of the ions to the nanotube under the influence of an external force, we use the following algorithm. The ions were initially kept at the minimum distance for which the SCF convergence of the system was obtained. It was found that K^+ ions can approach closest (∼1.9 Å) to the nanotube while the other ions come in the range of 2.0–2.3 Å. The system was then allowed to relax, with the ions free to move in the plane perpendicular to the nanotube axis. This resulted in the ions moving away from the nanotube surface because of the the inter-ionic electrostatic interactions. Fig. 1 shows the variation of the force acting on the system as a function of D. It can be seen that except Li^+, all other ions have a monotonically decreasing force as a function of distance. However, Li^+ shows a strong non-monotonic variation, with the minimum force at a distance of 2.9 Å. We do not have a clear understanding of this non-monotonic variation. It can also be seen from Fig. 1 that, though SCF convergence was obtained for K^+ at a distance smaller than other ions, Li^+ stabilizes at a closer distance (2.51 Å) under the influence of an external force. The equilibrium distances for the other ions were found to be much larger (Na^+: 5.5 Å, K^+: 5.6 Å, Cl^-: 5.3 Å, Br^-: 5.2 Å, I^-: 5.3 Å). This external force can be, for example, the electrochemical potential applied to the nanotube surface, as it is in the experiments [8–11]. An applied electrochemical potential of 2 V to the nanotube surface

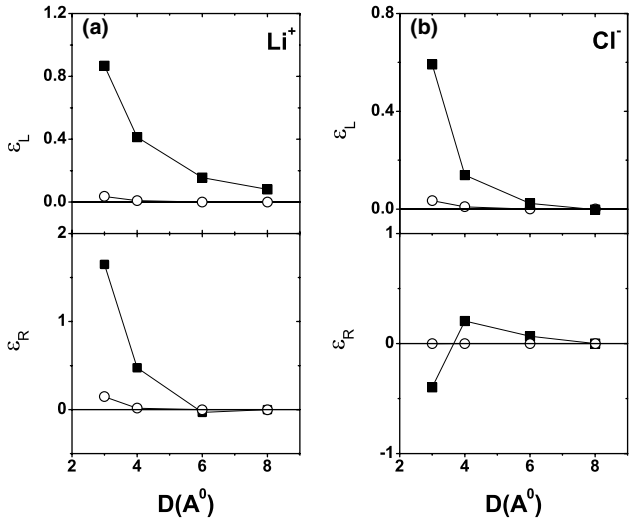

Fig. 2. The filled squares in the top panels show the axial strain, while in the lower panels show the radial strain developed in the nanotube due to the presence of (a) Li^+ and (b) Cl^-. The open circles show the contribution to the strain developed due to charge transfer alone.

translates to a force of about 0.25 nN on the ions in the Debye layer. This assumes that the entire potential drop occurs across the Debye layer of thickness ~10 Å formed at the nanotube–electrolyte interface modelled as a capacitor. We, therefore, chose the distances of the various ions corresponding to this force.

3.2. Strains developed in the nanotube due to the presence of ions

Having determined the equilibrium distances of various ions, we then froze the coordinates of the ions and let the previously optimized pristine nanotube coordinates relax to a new equilibrium geometry. The axial and radial strain parameters defined in terms of percentage changes for the nanotube are given by,

$$\varepsilon_L = \frac{(L - L_0)}{L_0} \times 100 \quad \text{and} \quad \varepsilon_R = \frac{(R - R_0)}{R_0} \times 100, \qquad (1)$$

where L_0 and R_0 are the equilibrium length and radius of the neutral, undistorted nanotube in the absence of ions. ε_L and ε_R in the presence of different ions kept at the equilibrium distances were calculated. It was found that Li^+ ions result in the maximum axial ($\varepsilon_L = 1.3$) and radial ($\varepsilon_R = 1.15$) strains in the nanotube, with the other ions producing a negligible effect ($\varepsilon_L < 0.2$ and $\varepsilon_R < 0.05$). This is a consequence of the greater proximity of the Li^+ to the nanotube surface as compared to the other ions. We then chose Li^+ cation and Cl^- anion for all further calculations involving varying the Li^+/Cl^--nanotube distance. ε_L and ε_R are shown by filled squares as a function of D for Li^+ and Cl^- in Fig. 2a and b, respectively. It can be seen that both axial and radial strain develops in the nanotube with the lowering of D for Li^+ as well as for Cl^-. The open circles show the

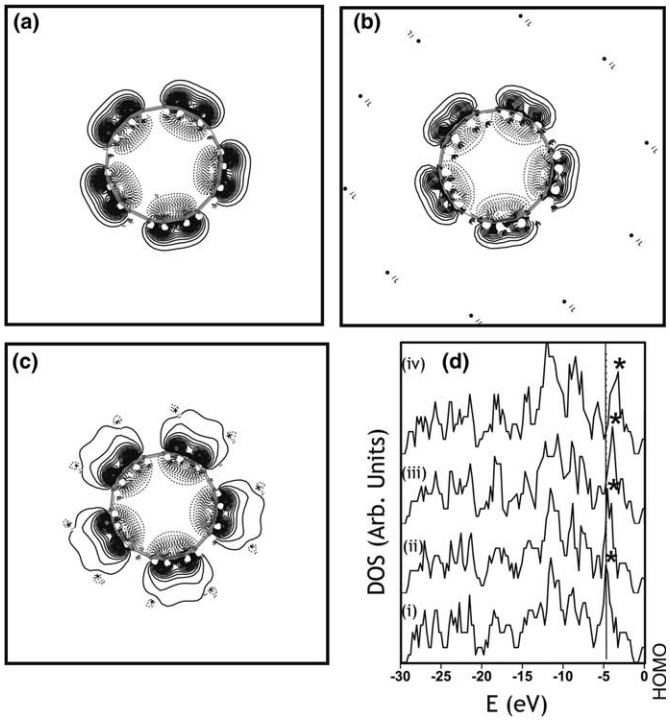

Fig. 3. Contour plots of a π orbital of A_g symmetry for the pristine tube (a), the tube with the Li^+ ions at $D = 6$ Å (b) and $D = 3$ Å (c). The plotting plane is perpendicular to the tube axis and contains a ring of Li^+ ions, (d) shows the DOS of the pristine nanotube (i), tube with the Li^+ ions at $D = 6$ Å (ii), $D = 4$ Å (iii) and $D = 3$ Å (iv). The zero of the graph is taken to coincide with the HOMO. The feature in the density of states, marked by * corresponds to the peak for the π orbitals.

contribution to the strain due to charge transfer alone (to be discussed later).

3.3. Effect of ions on the molecular orbitals of the nanotube

We now investigate the effect of the ions on the molecular orbitals of the nanotube. It is seen that for the pristine nanotube, the molecular levels are grouped in two bands. The band corresponding to π interactions occurs higher in energy, i.e., within ~6.5 eV from the HOMO, while the other band, mainly containing the σ interactions, occurs lower in the energy levels. When the ions are kept close to the nanotube, the electronic wavefunctions of the ions and the nanotube overlap. Fig. 3 shows the contour plot of a π orbital of A_g symmetry for the pristine tube (a), the tube with the Li^+ ions at $D = 6$ Å (b) and at $D = 3$ Å (c). The plotting plane is perpendicular to the tube axis and contains a ring of Li^+ ions. The solid lines show the bonding π orbitals while the dotted lines refer to the anti-bonding π orbitals. It can be seen that the molecular orbitals are considerably distorted for Li^+ ions at $D = 3$ Å. The distortions decrease as D increases. This is corroborated by quantifying the changes in the electronic density of states of the nanotube, which is plotted in Fig. 3d, for several ion-nanotube distances as well as for the pristine nanotube. It can be seen that the fine features related to the van Hove singularities are not captured by the calculations. We attribute the smearing of the van Hove singularities to the small number of unit cells considered in our calculation. The zero of the graph is taken to coincide with the HOMO. The feature in the density of states, marked by * in Fig. 3d at 4.4 eV, corresponding to the energy of the π orbitals, was found to shift towards higher energies, i.e., towards the HOMO, with the lowering of D. This is suggestive of the strong electrostatic interaction of the Li^+ ions with the π electrons of the nanotube.

3.4. Doping of the nanotube due to the presence of ions

The overlap of the electronic wave functions of the nanotube and the ions results in a redistribution of the charge density in the system, causing a partial transfer of hole (electron) from the cation (anion) to the carbon atoms of the nanotube. The average charge transfer per carbon atom of the nanotube, due to the overlap of the orbitals of the nanotube and the ions, is characterized by a parameter $\Delta q = \sum_{i=1}^{N} q_i/N$, where q_i is the charge on each carbon atom and N(=100) is the total number of C atoms in the nanotube segment. In the inset of Fig. 4a, Δq is plotted as a function of D for Li^+ (filled squares) and Cl^- (open circles). It may be noted that for similar values of D, the doping effects are greater for Li^+ than for Cl^-.

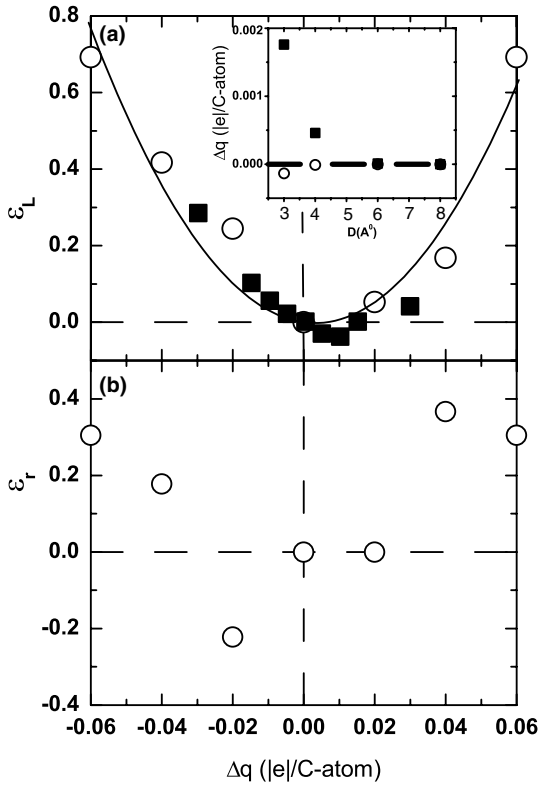

Fig. 4. (a) The Axial strains developed in the nanotubes due to electron and hole doping (open circles). The filled squares are obtained from the DFT calculations for (5,5) nanotube by Verissimo-Alves et al. [15]. The solid line is the fit to $\delta L/L = -a\Delta q + b|\Delta q|^2$, where $a = 2.6$ and $b = 6.5$ [15]. The inset shows the average charge (Δq) acquired by a carbon atom due to the presence of Li^+ (filled squares) and Cl^- (open circles) as a function of D. (b) Radial strains developed in the nanotubes due to electron doping and hole doping (open circles).

3.5. Doping induced strains developed in the nanotube

To estimate the contribution of the charge transfer alone to the strains developed in the nanotube, we optimize the structure of the nanotube (in the absence of ions) for different amounts of positive and negative charges on it. The strains ε_L and ε_R for both the electron and hole doping are shown in Fig. 4a and b, respectively. The obtained values of ε_L agree well with density functional calculations of the (5,5) tube (filled squares) taken from Verissimo-Alves et al. [15]. The data for the axial strain (Fig. 4a (open circles)) were fitted to the equation $\delta L/L = -a\Delta q + b|\Delta q|^2$, where $a = 2.6$ and $b = 6.5$ [15]. The contributions of charge transfer to the axial and the radial strains, as read out from Fig. 4 together with its inset, are plotted (open circles) in Fig. 2a and b. It is clear that the strains developed in the nanotube are primarily due to the electrostatic interaction of the ions with the π electrons of the nanotube. The charge transfer effects are rather negligible.

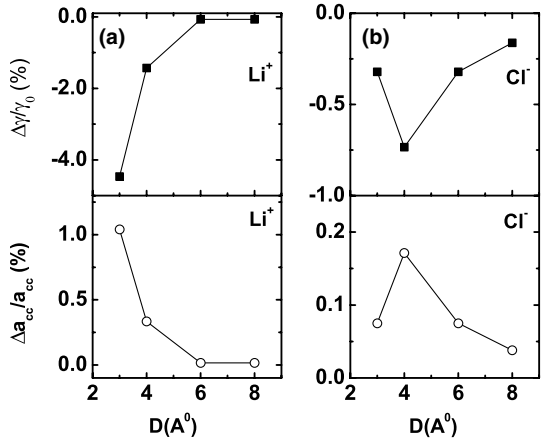

Fig. 5. The top panels show the percentage change in the overlap energy (γ), while the lower panels show the average percentage change in the nearest neighbor carbon–carbon distance (a_{cc}) due to the presence of (a) Li^+ and (b) Cl^-.

3.6. Change in γ due to the presence of ions

Since the nanotubes suffer combined axial and radial deformation, it is natural to expect that the average nearest neighbor carbon–carbon distance (a_{cc}) must be changing due to the proximity of the ions. This would, in turn, affect the orbital overlap between the adjacent carbon atoms. We have seen in Fig. 3 that π orbitals are most affected by the presence of ions. Thus, we look at the way the overlap energy (γ) between two adjacent $2p_z$ orbitals changes as a function of a_{cc}. Taking the functional form of the $2p_z$ atomic orbitals, we calculated the overlap integral as a function of distance (a_{cc}) between two adjacent carbon atoms. It was seen that it fits to the equation $\gamma(\Delta a_{cc}) = \gamma_0 \exp(-\Delta a_{cc}/a_0)$ where γ_0 is the overlap term for the pristine nanotube, $\gamma(\Delta a_{cc})$ is the modified overlap term when the equilibrium carbon–carbon distance changes by Δa_{cc}, and $a_0 = 0.33$ Å. Thus, for small values of Δa_{cc}, one obtains $\Delta\gamma/\gamma_0 = -\Delta a_{cc}/a_0$. The variation of the carbon–carbon bond length (a_{cc}) averaged over all the nearest neighbor carbon atoms is plotted as a function of D in the lower panels of Fig. 5a and b for Li^+ and Cl^-. It is interesting to note that the changes in the average value of a_{cc} and hence of γ is more pronounced for Li^+ as compared to Cl^- for $D = 3$ Å. The upper panels of Fig. 5a and b show the percentage variation of γ for Li^+ and Cl^-, respectively.

4. Conclusions

In this Letter, we show that the presence of ions near the nanotube surface has two effects on its electronic structure: (i) transfer of charge from the ion to the nanotube; (ii) electrostatic interactions between the delocalized π electrons of the nanotube and the ions. These effects are collectively responsible for the observed axial and radial strains in the nanotube. We show that the electrostatic interaction between the ions and the nanotube is the dominant mechanism in the generation of axial and radial strains. The change in γ brought about by changes in a_{cc} causes a rescaling of the energy gaps between a pair of van Hove singularities [8] and is responsible for the change in the Raman intensity seen in the in situ electrochemical experiments [8–11].

Acknowledgments

A.K.S. thanks the Department of Science and Technology (DST), Govt. of India, for financial support and Prof. C.N.R. Rao for fruitful collaborations. V.G. was supported by a KVPY fellowship awarded by DST, Govt. of India.

References

[1] A. Peigney, C. Laurent, E. Flahaut, R.R. Bacsa, A. Rousset, Carbon 39 (2001) 507.
[2] M. Eswaramoorthy, R. Sen, C.N.R. Rao, Chem. Phys. Lett. 304 (1999) 207.
[3] R.R. Bacsa, C. Laurent, A. Peigney, W.S. Bacsa, T. Vaugien, A. Rousset, Chem. Phys. Lett. 323 (2000) 566.
[4] S. Ghosh, A.K. Sood, N. Kumar, Science 299 (2003) 1042.
[5] J. Kong, N.R. Franklin, C. Zhou, M.G. Chapline, S. Peng, K. Cho, H. Dai, Science 287 (2000) 622.
[6] P.G. Collins, K. Bradley, M. Ishigami, A. Zettl, Science 287 (2000) 1801.
[7] R. Baughman, C. Cui, A. Zakhidov, Z. Iqbal, J.N. Barisci, G.M. Spinks, G.G. Wallace, A. Mazzoldi, D.D. Rossi, A.G. Rinzler, O. Jaschinski, S. Roth, M. Kertesz, Science 284 (1999) 1340.
[8] S. Ghosh, A.K. Sood, C.N.R. Rao, J. Appl. Phys. 92 (2002) 1165.
[9] L. Kavan, P. Rapta, L. Dunsch, Chem. Phys. Lett. 328 (2000) 363.
[10] L. Kavan, P. Rapta, L. Dunsch, M.J. Bronikowski, P. Willis, R.E. Smalley, J. Phys. Chem. B 105 (2001) 10764.
[11] P. Corio, P.S. Santos, V.W. Brar, G.G. Samsonidze, S.G. Chou, M.S. Dresselhaus, Chem. Phys. Lett. 370 (2003) 675 and references therein.
[12] K. Okazaki, Y. Nakato, K. Murakoshi, Phys. Rev. B 68 (2003) 035434.
[13] S. Gupta, M. Hughes, A.H. Windle, J. Robertson, J. Appl. Phys. 95 (2004) 2038.
[14] S. Kazaoui, N. Minami, N. Matsuda, H. Kataura, Y. Achiba, Appl. Phys. Lett. 78 (2001) 3433.
[15] M. Verissimo-Alves, B. Koiller, H. Chacham, R.B. Capaz, Phys. Rev. B 67 (2003) 161401 (R).
[16] C.T. Chan, W.A. Kamitakahara, K.M. Ho, P.C. Eklund, Phys. Rev. Lett. 58 (1987) 1528.
[17] P. Keblinski, S.K. Nayak, P. Zapol, P. Ajayan, Phys. Rev. Lett. 89 (2002) 255503.
[18] M. Verissimo-Alves, R.B. Capaz, B. Koiller, E. Artacho, H. Chacham, Phys. Rev. Lett. 86 (2001) 3372.
[19] M.W. Schmidt, K.K. Baldridge, J.A. Boatz, S.T. Elbert, M.S. Gordon, J.H. Jensen, S. Koseki, N. Matsunaga, K.A. Nguyen, S.J. Su, T.L. Windus, M. Dupuis, J.A. Montgomery, Comput. Chem. 14 (1993) 1347.
[20] A. Kalra, S. Garde, G. Hummer, Proc. Natl. Acad. Sci., USA 100 (2003) 10175.
[21] L.G. Bulusheva, A.V. Okotrub, D.A. Romanov, D. Tomanek, J. Phys. Chem. A 102 (1998) 975.